ALMA MATER STUDIORUM
UNIVERSITÀ DI BOLOGNA

ARCHIVIO ISTITUZIONALE
DELLA RICERCA

Alma Mater Studiorum Università di Bologna
Archivio istituzionale della ricerca

Damage and collapses in industrial precast buildings after the 2012 Emilia earthquake

This is the final peer-reviewed author's accepted manuscript (postprint) of the following publication:

Published Version:
Savoia, M., Buratti, N., Vincenzi, L. (2017). Damage and collapses in industrial precast buildings after the 2012 Emilia earthquake. ENGINEERING STRUCTURES, 137, 162-180 [10.1016/j.engstruct.2017.01.059].

Availability:
This version is available at: https://hdl.handle.net/11585/583152 since: 2017-03-27

Published:
DOI: http://doi.org/10.1016/j.engstruct.2017.01.059

Terms of use:

Some rights reserved. The terms and conditions for the reuse of this version of the manuscript are specified in the publishing policy. For all terms of use and more information see the publisher's website.

This item was downloaded from IRIS Università di Bologna (https://cris.unibo.it/).
When citing, please refer to the published version.

(Article begins on next page)

12 October 2024

This is the final peer-reviewed accepted manuscript of:

Marco Savoia, Nicola Buratti, Loris Vincenzi, ***Damage and collapses in industrial precast buildings after the 2012 Emilia earthquake****, Engineering Structures, Volume 137, 2017, Pages 162-180, ISSN 0141-0296*

The final published version is available online at:
https://doi.org/10.1016/j.engstruct.2017.01.059

Rights / License:

The terms and conditions for the reuse of this version of the manuscript are specified in the publishing policy. For all terms of use and more information see the publisher's website.

This item was downloaded from IRIS Università di Bologna (https://cris.unibo.it/)

When citing, please refer to the published version.

DAMAGE AND COLLAPSES IN INDUSTRIAL PRECAST BUILDINGS AFTER THE 2012 EMILIA EARTHQUAKE

Marco Savoia, Nicola Buratti

DICAM – Structural Engineering, University of Bologna, Bologna, 40136 Italy, marco.savoia@unibo.it

Loris Vincenzi

DIEF – University of Modena and Reggio Emilia, Modena, 41125 Italy, loris.vincenzi@unimore.it

SUMMARY – The present paper presents a complete and commented collection of cases of damage and collapse in reinforced concrete (RC) precast industrial buildings, observed by the authors during a series of field surveys after the 2012 Emilia earthquake in Northern Italy. They were selected among a total of about 2000 industrial RC precast buildings, whose structural characteristics and damage have been collected in a large database by the authors.

The main causes of the collapses were vulnerabilities related to the structural characteristics of Italian precast buildings not designed with seismic criteria. In particular, these structures were typically built as an assembly of monolithic elements (roof elements, main and secondary beams, columns) in statically determinate configurations. The most common failure causes identified were: the absence of mechanical connectors between precast monolithic elements, the interaction of structural elements with non-structural walls, the insufficient column bending capacity, the rotation of pocket foundations, the inadequacy of connections of external precast cladding walls to bearing elements (columns and beams), the overturning of racks in buildings used as warehouses or in automated storage facilities.

Key words: earthquake collapses, industrial buildings, precast technology, connection systems.

1 INTRODUCTION

A series of strong earthquakes struck the Emilia region, in Northern Italy, in May 2012. Two main earthquakes can be identified in the seismic sequence, with mainshocks featuring similar energies: the first event with moment magnitude, $M_w = 6.1$, struck on May 20th, while the second, with $M_w = 6.0$, on May 29th. The May 20th earthquake caused the collapse of several RC precast buildings in the industrial areas of S. Agostino, Bondeno, Finale Emilia, S. Felice sul Panaro, while the May 29th earthquake was particularly severe for industrial buildings in Mirandola, Cavezzo and Medolla. In the industrial areas close to the epicentres (less than 5 km), according to some estimates, more than 60 % of RC precast buildings collapsed or were severely damaged [1]. Also other types of buildings, such as cast-in-place RC and masonry structures, were designed for non-seismic loads only and were significantly damaged. Historical city centres were also damaged, being built according to practical construction rules only (in the pre-code era).

No seismic design rules were mandatory in the area until the last decade, even if, in the past, the region had experienced earthquakes with similar magnitudes, such as the 1570–1574 Ferrara earthquake [2]. Only in 2003, an updated seismic hazard map for Italy classified the Emilia region as a low-to-moderate seismicity area [3]. That hazard map was formally adopted in 2003 [4], becoming mandatory for designers only in 2008 [5]. For these reasons, most of the industrial buildings in the area had been built without any seismic-design rule [6]. In particular, precast buildings were typically constructed as an assembly of monolithic elements (roofing elements, main and secondary beams, columns) in simply supported conditions, without mechanical connectors. Often, neoprene pads were used to allow end rotations in long span beams, thus further reducing friction resistance. According to Bellotti et al. [7] 85% of the precast buildings in the Emilia region were built without seismic design rules and more than 70% featured friction-based connections. Overviews on the main typologies of prefabricated structures used in Italy since the 70s are provided by Bonfanti et al. [8] and Mandelli, Contegni et al. [9]. The most common precast industrial buildings in the area of interest were single-storey statically-determined frame structures with pocket

foundations [10]. The seismic behaviour of these structures, as discussed by Bellotti et al. [7], is characterised by great flexibility and large displacements.

Damage and collapses of precast buildings were observed by many authors after past earthquakes all over the world [11–17] and in Italy [18], but the extent and the severity of the collapses after the Emilia earthquakes are unprecedented in Italy. The first field reports on the Emilia earthquakes ([6,19–21]) showed that many collapses were caused by the lack of mechanical connectors between structural elements. In particular, Bournas et al. [21] reported that 25% of the damaged buildings that they analysed presented a partial or total collapse of the roofing elements, mainly due to the unseating of the main girders. Similarly, Liberatore et al. [20] observed the unseating of shed beams (used as roofing elements) in almost 30% of the 30 buildings that they analysed. Savoia et al. [19] highlighted the effects of the interaction with non-structural elements, like masonry or concrete panels, in particular when these latter were irregular.

The present paper comprises two parts. A discussion on the main features of the ground-motions recorded during the seismic sequence is presented first, highlighting those that might have been particularly critical for prefabricated structures. In particular, near-field effects such as pulse like behaviour and directionality are discussed with more details, since they were not analysed in the literature concerning the Emilia earthquakes. Then, the paper provides a complete and commended collection of damage cases and failure modes observed by the authors during the field surveys that took place in the zones struck by the earthquakes. The surveys in S. Felice sul Panaro and S. Agostino were carried out after the May 20th earthquake, while those in Mirandola, Cavezzo and Medolla after both mainshocks. The damaged or collapsed buildings illustrated in the paper were selected among a total of about 2000 industrial RC precast buildings, whose damage has been collected in a large database periodically updated [1,22]. In all the cases the main reasons of the collapses were identified in relation with the usual design criteria for non-seismic zones adopted in the region, which lead to structures with intrinsic vulnerabilities [7].

2 FEATURES OF THE GROUND MOTIONS

The present section describes the main features of the strong ground-motions recorded during the seismic sequence. Various near-source effects such as high vertical accelerations and pulse-like features could be observed in some of the records and might have significantly contributed to the final damage scenario. In fact, near source ground-motions are in general more demanding on structures than far-field motions [23–26].

On May 20th, 2012, a M_w = 6.1 [27] (epicentre at latitude = 44.89° N and longitude = 11.23° E) earthquake struck the area in the Po River Valley, north of the city of Modena, Italy. In the following 13 days, five M_w > 5 events occurred (see Figure 1). Among these, the most intense was a M_w = 6.0 [27] earthquake on May 29th, with epicentre located about 12 km West of the first mainshock (latitude = 44.85° N and longitude = 11.09° E). This event can be considered as a second mainshock.

In the recent past, the same area was struck in 1996 by a M_w = 5.4 earthquake and by other smaller earthquakes in 1986 and 1967. The most destructive historical events were the November 15th, 1570, Ferrara earthquake, with an estimated M_w = 5.48, and the March 17th, 1574 event (M_w = 4.7), that produced damage in Finale Emilia [2,28].

The seismic-tectonic structure of the area is characterized by the northern Apennines frontal thrust systems, composed of a pile of North-East verging tectonic units as a consequence of the collision between the European plate and the Adria plate [29]. The geometry of the thrusts below the Po Valley has been studied by various authors [30,31]. Three major curved thrust fronts are identified, as depicted in Figure 2: the Monferrato, the Emilia, and the Ferrara-Romagna Arcs. Active NE-SW shortening has been documented by various authors [32,33].

Several ground-motion recording stations of the Italian strong-motion network [34] recorded the ground-shaking during the 2012 earthquake sequence. Furthermore, after the first mainshock a number of temporary recording stations were installed (see Figure 3). Site classification data are not available for all

the recording stations but, to the authors knowledge, EC8 C class can be reasonably assumed in the whole area [35]. The ground-motion records analysed in the present paper were obtained from the ITACA database [36,37], which contains processed accelerograms mostly recorded in Italy [38].

During 2012 Emilia earthquakes, horizontal Peak Ground Accelerations (PGA_h) up to 259 cm/s^2 (May 20th, MRN station, epicentral distance R_e = 12.3 km) and 411 cm/s^2 (May 29th, MIR01 station, R_e = 1.4 km) were recorded. Horizontal pseudo-acceleration (PSA_h) response spectra, computed for the two horizontal components (East-West and North-South) of the ground-motions recorded by the stations closest to the epicentres, are depicted in Figure 4. Figure 4a shows that, during the May 20th earthquake, large pseudo-accelerations were recorded at the MRN station (R_e = 12.3 km) in the 0.5-1.0 s period range, possibly because of site-response and near-field effects, as discussed later. PSA_h response spectra reported in Figure 4b for the May 29th event confirm large accelerations in the 0.5– 1.0 s period range. Furthermore, the spectra for the North-South recordings at the MIR01 (R_e = 1.4 km) and MRN (R_e = 4.1 km) stations feature a peak at T =1.5 s [7]. Also in this case, in addition to site effects, near-source effects have probably contributed to the definition of the spectral shape [39]. The possible effect of site response was suggested by Priolo, Romanelli et al. [40], who analysed eight different locations in the region struck by the earthquakes using the horizontal-to-vertical spectral ratio method (HVSR) and the spatial autocorrelation method (ESAC) [41]. All the sites investigated showed similar HVSR characteristics, in particular, a broad peak of fundamental resonant frequency in the low frequency band 0.5-1.5 Hz. According to Priolo, Romanelli et al. that peak was due to the geological structure of the sites, characterized by superficial cohesionless soils, with very low shear-modulus values, and by a weak S-velocity contrast at a depth of 80 to 100 m. The importance of site response was confirmed also by Gallipoli et al. [42]. This peak in the pseudo acceleration spectra may have played an important role in the collapse of recent prefabricated structures (see Section 4) because their first natural period belongs to that range [43,44].

Some of the ground-motions recorded presented typical near-field features. Thanks to the large number of temporary recording stations close to the epicentre of the May 29th event, very large vertical

peak ground accelerations were recorded (up to 841 cm/s^2). As expected, vertical ground-motions featured a faster attenuation over distance than horizontal ground-motions. Vertical *PSA* response spectra are reported in Figure 6. They feature very large pseudo accelerations at very short periods, i.e. $T < 0.1$ s. These accelerations have played a role in the collapse of industrial precast structures made of monolithic elements with beam-column connections based on friction resistance (see Section 5), as indicated by the numerical simulations performed by Biondini et al. [45] and Liberatore et al. [20]. Furthermore, they might have, to a smaller extent, partially affected the stability of columns by increasing vertical loads therefore producing larger second order effects.

Pulse-like features [23,25,26] could be identified is some records as well. Using the criterion proposed by Baker [46], it is possible to classify as pulse-like the ground-motion records listed in Table 1. The scientific literature indicates that pulse-like ground-motions lead to larger nonlinear displacement demands when compared to non-impulsive records with similar elastic response spectra [47,48]. These large displacement demands might have contributed to some failures, such as the unseating of beams, which are dominated by friction and displacement demands.

Finally, the recordings from the stations closest to the epicentres are analysed in order to evaluate ground-motion directionality. Directionality can be quantified by calculating PSA_h values for various azimuth angles θ. Periods from 0.0 s to 3.0 s are considered. Figure 5

$$\alpha = PSA_h(T_i, \theta) / \max_{\theta}(PSA_h(T_i, \theta))$$

$$\max_{\theta}(PSA_h(T_i, \theta))$$

the segment connecting the location of the ground-motion recording station to the epicentre. Finally, it is worth noticing that is not possible to clearly identify a direction for which all the PSA_h are maxima.

3 CODE PRESCRIPTIONS IN THE REGION FOR DESIGN OF PRECAST RC STRUCTURES

This section presents an overview of code provisions for precast RC structures in the areas affected by the earthquake. In the following, it will be shown that most failures were a direct consequence of the lack of application of seismic design rules, such as incorrect structural detailing of columns and lack of adequate connections between monolithic elements. The region struck by the earthquake was in fact not classified as a seismic area at the time of construction of most of the buildings and, in agreement with the national codes at that time, precast concrete buildings were generally designed to bear only vertical loads, and, as the only horizontal loads, wind and crane actions when relevant.

3.1 Evolution of seismic hazard maps

The first seismic hazard map for Italy was issued after the destructive Messina earthquake in 1908. In the following years, several updates were implemented, typically after the occurrence of destructive earthquakes. The most significant improvement was achieved in 1996 [49], when Italian municipalities were classified into four seismic zones, corresponding to different seismic hazard levels: the first zone was characterized by the largest value of horizontal seismic actions, while for the fourth zone no seismic actions were prescribed for design. The Emilia region was mostly classified as non-seismic, with the exception of some upland areas (far from the areas struck by the 2012 earthquakes). The seismic hazard map was then significantly updated in 2003 [4] and 2008 [5]. The new map was based on a probabilistic seismic hazard assessment which significantly increased the number of municipalities classified as seismic areas. Almost the entire Emilia region is presently classified as a low-to-medium hazard zone. With reference to a 475

years return period, the current hazard map predicts PGA_h values ranging from 0.14g to 0.17g on rock soils, and 0.22g - 0.26g on C class soft soils, such as those in the area hits by 2012 earthquakes.

3.2 Evolution of building codes for RC precast structures

The first complete law prescribing design rules for RC structures in non–seismic regions dates back to 1971 (N. 1086, November 5th, 1971), followed in 1974 by the first law (N. 64, February 2nd, 1974) regulating the design of structures in seismic regions. These laws did not contain specific provisions for precast structures.

The 1976 Friuli earthquake (North-Eastern Italy) produced extensive damage and some local failures of industrial buildings, which exhibited all the critical issues typical of structures built without proper seismic design criteria. After this earthquake, a sequence of decrees and guidelines were published. Among them, the most important documents, concerning the design of precast RC structures, were the CNR 10025/84 [50] guidelines and the DM 3 December 1987 [51] decree. The CNR 10025/84 guidelines defined the basis of design for precast concrete structures as well as requirements on materials, manufacturing processes and end products (manufacturing tolerances and dimensions, surface quality, etc.). For some elements, typical of precast structures (pocket foundations, corbels, etc.), detailed design procedures were defined. For all other structural elements, such as beams and columns, only general rules were given, referring to further national codes for details on design, minimum dimensions or reinforcement ratios. The CNR 10025/84 guidelines also defined specific rules for the design of connections between monolithic elements (rubber bearings, steel connectors and dowels, etc.). The use of dowels to connect precast beams with columns was clearly recommended in seismic areas.

Three years later, the 3 December 1987 Decree defined the basis of design for precast concrete structures in seismic areas; the use of simply supported bearings or friction-based supports without mechanical connectors was forbidden. Of course, those prescriptions were mandatory only in municipalities

belonging to areas classified as seismic, whereas in non-seismic municipalities, as those struck by the May 2012 earthquakes, beam-column connections based on friction were still allowed.

In the following years, several decrees were issued to update design criteria for concrete structures. The 14 February 1992 [52] and the 9 January 1996 [53] decrees defined requirements for the design of normal and prestressed RC structures in non-seismic areas, indicating design rules, verification criteria, and detailing prescriptions. The 16 January 1996 [49] decree defined new design criteria for earthquake resistant structures. Of course, these rules were not mandatory in municipalities interested by the May 2012 earthquakes. From the analysis of damage and collapses presented in Sections 5 and 6, it clearly emerges that precast concrete structures designed for vertical loads only were often inadequate to support the horizontal seismic actions.

4 TYPES OF PRECAST BUILDINGS IN THE REGION

This section presents a classification of the main prefabricated building typologies in the area. This classification will allow a better understanding of the causes of damage and collapses described in detail in the following sections.

The region struck by the earthquakes is one of the most productive areas in Italy. The development of industrial zones, at least one for each municipality, started in the late sixties. These zones expanded until a few years ago, before the economic crisis that hit the construction sector in Italy in 2008. The typical layout of a single-storey industrial building is composed of a series of basic portal frames, realized as the assembly of monolithic precast elements. Each frame has precast cantilever columns clamped in pocket foundations, and precast concrete roof girders supported over the columns. Precast slab elements are also simply supported over the roof beams. In the case of structures not designed with seismic provisions, the beam-column and slab-beam connections were typically friction-based, without mechanical connection devices. Furthermore, often neoprene pads were used in order to allow beam end rotations under vertical loads. The stability of these structures and their ability to withstand horizontal actions depend on the

cantilever behaviour of columns and on friction resistance of supports. Compared to cast-in-place RC frame structures, they completely lack structural redundancy and, therefore, have no redistribution capacity.

During the field surveys, different precast technologies were identified. With a few exceptions, they can be classified according the following two categories:

- Type 1 - Buildings with double slope precast beams simply-supported at the top of the columns. A typical technology adopted in the 70's and the 80's, and also recently for small and cheap constructions, for instance for agricultural warehouses;
- Type 2 - Buildings with planar roof, composed of long-span prestressed roof or floor elements simply-supported on (prestressed or not) precast girder beams. This technology was widely used after the 80's, typically for large industrial facilities. It allows also the realization of construction with two or more floors.

Both typologies might have different types of precast roofing or slab elements, depending on the spans, as well as on insulation and lighting requirements. Following the technical developments of the precast-technology, the two types of structures were very different in terms of dimensions, spans, and masses of the elements, and were designed according to different criteria. For these reasons, as will be discussed in the following Sections, each typology exhibited specific damage and failure modes.

Type 1 industrial buildings typically have rectangular plan with the main frames in the direction of the short side. Frames have normally double slope precast beams with spans from 12 m to 20 m. The distance between frames is 6 – 10 m (Figure 7). The roof can be made of precast elements with hollow clay blocks or, in recent constructions, TT or hollow-core concrete elements. Columns are usually quite slender, featuring 30 – 40 cm wide square cross-sections. These buildings typically have masonry infills, all around the perimeter, providing strength and stability for wind loads (the only horizontal action considered at the time of construction). There are no mechanical connectors in beam-column joints. The depth of the cross-section of the main beams can be up to 2 m at mid-span. Beams typically feature either no or little restraints against out-of-plane movements, with the exception of upper pocket supports (named forks) at the top of

columns. These buildings have normally a single storey, eventually with an intermediate floor in a limited portion of the building on one side (see Figure 7a), where offices are typically located. Often, the presence of that intermediate floor on one side of the building caused an irregularity in the structural behaviour, with negative effects during ground motions.

Type 2 precast buildings with planar roof are larger in plan that Type 1 structures. They are typically designed to obtain large empty spaces with only a few columns inside (see Figure 8). Planar precast RC girders (e.g., I- or omega-shaped beams) are supported on columns. In order to achieve long spans also in the slab direction, different kinds of prestressed elements are adopted for roofs or slabs, such as TT, Y-shaped, or shed profiles. More recently, the use of precast vaulted thin-web elements (called "wing profiles") allowed to cover roof spans as long as 30 m (Figure 8b). In this case, curved panels made of glass or transparent polycarbonate are placed between the structural thin-web roof elements with the purpose of lighting the interior of the building. When this solution is adopted, quite commonly in the last 20 years for large industrial buildings (spans longer than 20 m in both directions), the roof is of course highly deformable in its plane. RC columns have large rectangular cross-sections (with sides up to 60-80 cm) and must bear both vertical and horizontal loads. In fact, cladding walls are RC panels, externally fixed to the columns and the upper beams, and expected to have no structural function.

5 DAMAGE AND COLLAPSES IN INDUSTRIAL BUILDINGS WITH DOUBLE SLOPE PRECAST BEAMS (TYPE 1)

This section and the following present a commented collection of failure cases in precast RC buildings found during the field surveys. The locations of the buildings described in the following are indicated in Figure 9. Each building is identified by a number, which is also indicated in all the following figures. The main weaknesses of Type 1 buildings are highlighted and discussed here.

5.1 The structural behaviour of regular buildings

Buildings with double slope precast beams were typically designed for vertical loads only, and stability against horizontal loads due to wind was provided by masonry infills. Quite often columns featured two deep grooves along the height to improve the connection with the infills. Columns typically had small cross-sections with the minimum longitudinal steel reinforcement allowed by the codes. Therefore, the effect of the in-plane stiffness of masonry infill-walls was very important being, in general, much larger that the column stiffness.

Buildings with regular infill walls all around the perimeter, and in-plane rigid roofs, rarely suffered serious damage, being the strength of the walls in general sufficient to resist the horizontal forces induced by ground motions. Of course, in this case, the rigid diaphragm behaviour of the roof is fundamental for transferring horizontal actions to walls. In most cases, only minor damage was detected in the masonry walls (Figure 10a) or in the forks on the top of columns (Figure 10b). This damage was caused by the lateral rotation of main beams due to the vertical eccentricity of the roof mass with respect to the supports. Even if not designed to carry horizontal actions, and in spite of their very light steel reinforcement, forks played, when present, a very important role in restraining beam lateral rotation and, consequently, the possible roof collapse. Only in a few cases, buildings with regular infill walls collapsed. These structures typically had deformable roofs, not able to properly transfer lateral seismic forces to the perimeter walls. In the building depicted in Figure 11a, the roof was made of non-structural plastic roof elements, and the horizontal seismic forces acting in the transverse direction of the building were not effectively transferred to the two facade masonry walls (located along the two short sides in plan). The building then collapsed because of overturning of the longer-infill walls, with the masonry panels on the short sides mostly undamaged.

In very economical structures, such as shelters in livestock farms, roofs were often made of double-slope precast beams with secondary RC purlins carrying light sandwich roof panels. In these case, the roof was very deformable and, in particular for seismic actions perpendicular to main precast beams, was not able to provide the necessary in-plane stiffness to avoid the lateral deformation of beams. In a livestock

shelter, a laser scanner survey (Figure 11 b) was performed after the earthquake. Large permanent displacements (up to 20 cm) and rotations of the beam cross-sections (red lines) were measured.

5.2 The role of irregularities in external masonry infill walls

Industrial buildings with curtain masonry walls and strip-windows just under precast double-slope beams were often severely damaged and often collapsed (Figure 12). This was probably the most frequent cause of failure in some industrial areas (e.g., San Felice sul Panaro and Mirandola).

In many cases, the interaction of transverse walls (along the short side of buildings) with precast columns caused a loss-of-support failure of the main beams of the two end frames. In fact, when the roof oscillates laterally, the deformation of columns moving against walls (i.e. one column at each facade of the building) is restrained by the interaction with these latter, producing a short-column effect. This circumstance can be easily explained with a simple example.

A general terminal frame with two base-clamped columns and a simply supported precast beam is depicted in Figure 13a. Considering the presence of a flexible roof, the weight of the roofing elements corresponding to the frame tributary area is indicated with W, and the total seismic lateral force is $A \cdot W$, where A indicates the pseudo spectral acceleration (PSA_h) at the natural period of the frame, in units of g, i.e., $A = PSA_h/g$. Without the infill wall (as in the case of a central frame), this force will be equally distributed between the two columns. Therefore, at the beam supports, the horizontal-to-vertical force ratio is $H/N = A \cdot W/A = A$. Sliding of beams from their supports occurs if H/N=A is be larger than the friction coefficient, which can be assumed of the order of 0.5 for a concrete-concrete support (without neoprene pads) [54]. That value was usually not exceeded, at least for frames oscillating with a period typically in the range 1.2 ÷ 1.5 s. Considering the pseudo-acceleration spectra in Figure 4, for T= 1.2 ÷ 1.5 s, $A = PSA_h/g$ is about 0.4, i.e. smaller than the friction coefficient. On the contrary, considering an infilled frame with a strip window (Figure 13b) and assuming that the roof is moving in the right direction, because of the interaction with the infill wall most of the lateral force will be acting on the left column. As an example, if

the height of the infill is 2/3 L, assuming that the infill can be modelled as a rigid compression strut, the lateral stiffness of the left column will be about 20 times larger than that of the right column (Figure 13c). Therefore, the maximum H/N ratio on the left column is approximately $H/N = 2A'$, being $A' = PSA'_h/g$ and PSA'_h the pseudo spectral acceleration at the natural period of the infilled frame, much shorter than the natural period the bare frames (about 0.2÷0.4 s). For periods in that range, A' can be up to 0.8 ÷ 1.0 (see Figure 4) and then $H/N = 2A' = 1.6 \div 2.0$, i.e., up to 4 times greater than the friction coefficient, causing certainly the unseating of the precast beam. Horizontal forces in columns of the infilled side frames can be even greater in the presence of a roof with some in-plane stiffness, because most of the horizontal force related to the mass of the entire roof is transferred to the two columns of the end frames interacting with the infilled walls.

In the building in Figure 12b, it is interesting to note that, in the bay on the left side, the presence of an irregular wall caused the unseating of the double-slope beam, whereas, in the bay on the right side, the masonry wall, only partially restrained by the RC structure, collapsed and, consequently, no unseating of the roof beam occurred. Typically, this kind of failure involved only the two external portal frames (Figure 12a, b), and in a few cases also the subsequent ones (Figure 12c). In the building of Figure 12d, the presence of a rigid partition masonry wall inside the building caused the same kind of collapse. Because of the action in the infill wall, the horizontal force in the short columns of the terminal frames was so high that, when the loss–of–support failure did not take place, flexural plastic hinge failures were observed (Figure 14b-c) in the columns. In some cases, the significant reduction of the shear-span of columns, due to the interaction with infills, produced a modification of the failure mode from flexural to shear-type, as illustrated in Figure 14a which shows a flexural-shear failure.

The interaction of the portal frame elements with additional façade RC elements often caused severe damage or even collapses. Figure 15 shows a collapse mainly caused by the presence of an additional RC facade column, aimed at supporting a metallic gate, and connected at the mid–span of the precast beam of the portal frame. Of course, the double slope beam was originally designed neglecting the presence of the

additional facade column, i.e., a simply supported condition. Being instead in a statically redundant condition (three–point support), the double – slope beam suffered sudden variations of the vertical reactions on the two lateral supports on the main external columns during the earthquake. The condition of overcoming of friction resistance was then attained during the ground–motion and the support was lost on the right column. Of course, with half beam behaving as a cantilever, failure occurred because of insufficient top steel-reinforcement.

Plan-irregularity was another important cause of roof collapses. For instance, in the building of Figure 16a, the presence of a smaller (and then stiffer) precast building on the right side caused the transmission of high horizontal forces at the support levels of intermediate columns. Friction resistance at the beam-column support was then overcome and all the intermediate beams fell down from their supports. The prefabricated building in Figure 16b suffered the collapse of the roof of a bay external to the two main spans of the building, being much more flexible and undergoing large and differential displacements at the level of column tops.

In some cases, masonry walls, not connected to the top beam because of the presence of strip windows, either collapsed or were severely damaged (Figure 17a). Moreover, Figure 17b shows a partial collapse of a roof made of clay hollow block panels supported over curved precast RC beams. This structural typology, used frequently in the late sixties for buildings hosting manufactories, has masonry walls of different height along both the long and short sides carrying the horizontal seismic forces. These very flexible, and lightweight, roofs were usually able to deform during the ground motions without significant damage. Only in a few cases, as in the building of Figure 17b, the relative displacement between the last two curved RC beams of the roof at the building extremities, caused damage and sometimes collapse of portions of the clay hollow block panels of the roof. In fact, the displacement of the façade RC beam is clearly limited by the infill walls, while the displacement of the following beam is much larger because of roof flexibility.

6 DAMAGE AND COLLAPSES IN MODERN INDUSTRIAL BUILDINGS WITH FLAT ROOFS (TYPE 2)

This section presents a commented collection of failure cases observed on Type-2 buildings. The failure mechanisms in more recent precast industrial buildings with flat roofs are various and more complex with respect to those described in the previous section. Even some recent structures (built in the last 10 years) suffered extensive damage of even full collapses (Figure 18).

6.1 Unseating of roof elements

In many cases, partial collapses were related to the unseating of roof elements, even without any evident damage in columns. In fact, roof precast elements were typically not restrained to precast beams, with the interposition of neoprene pads that reduced friction resistance [55]. Especially in the case of precast elements alternated with roof-lights, the roof in-plane stiffness was negligible and columns were free to oscillate as independent cantilevers. Then, the significant, and possibly even out-of-phase, relative displacements between the columns caused the unseating failure of roof elements from beams or of beams from columns. The loss–of–support failure of roof elements often occurred in zones corresponding to plan irregularities of buildings, such as variations in the number of spans of the frames (Figure 19a and the building on the left of Figure 19b). In other cases, the loss–of–support failure occurred in the central part of buildings, as in the building on the right of Figure 19b. This type of failure was facilitated by the non-rigid in-plane behaviour of the roofing elements which led to large relative movements. According to some studies [45], inertia forces produced by the large vertical accelerations that affected the near-source areas might have contributed to these failures by modifying vertical loading and the corresponding friction resistance.

In some cases, despite of their presence, steel dowels to connect beams and columns were inadequate to bear the forces to be transferred. In Figure 20a, the steel reinforcement in the rear portion of the beam was not sufficient to resist the force produced by the steel dowel in the beam-column connection. Figure

20b shows a detail of the top of a column in a building designed according seismic rules. A horizontal steel dowel can be seen. It was used to connect the omega-shaped precast beam the column. Nevertheless, because of plan irregularity, the action in the connection was larger than calculated in design, the 22 mm diameter dowel was insufficient and the beam fell down from its support. The dowel can be seen completely bent in the picture.

Figure 21 shows a large fruit warehouse serving several municipalities in the area. The roof structure was made of inclined precast beams forming a shed structure. Some beams fell down from the lower support, being the underlying column shorter (and then stiffer) than the column under the upper support. Most of the horizontal force was then transferred at the level of the lower support and, in some cases, the friction resistance was exceeded.

In the case of the precast multi-storey commercial building of Figure 22, the loss of support of precast roof elements was also due to plan-irregularity. The larger lateral stiffness of the right portion of the building caused the transfer of large horizontal forces at the level of the roof–beam supports, with forces exceeding friction resistance.

Some roof collapses were caused by the lateral rotation of beams supporting roof elements. These rotations were due to the eccentricity of the upper mass of the roof with respect to the beam supports. In the building of Figure 23a-b, most of the roof collapsed due to the rotation of the beam that followed the rupture of upper forks of columns, whose steel reinforcement was clearly insufficient. In other cases, the upper fork was even absent (see Figure 24a). In the collapsed structure of Figure 24b, the lateral rotation of the beams during the earthquake is highlighted by the shear cracking of the lower portion of the beam.

6.2 Failure of internal columns

Many collapses in recent precast buildings were related to the failure of some internal columns and, in these cases, very large portions of buildings were involved in the collapse.

The building in Figure 25a is particularly representative of this type of failure. Significant damage was registered in internal columns after the May 20th earthquake, and the building fully collapsed during the May 29th earthquake. This structure was particularly vulnerable to horizontal seismic actions, as many other similar recent precast construction designed without specific seismic provisions, the only actions considered being gravity and wind loads. In design of these structures, the wind lateral forces were mostly assigned to external columns, being the roof fully deformable due to the presence of large roof-flight strips between the slab precast elements. According to the design criteria adopted, internal columns had resisting bending moments smaller than external columns, being the moment in the first ones only that corresponding to the eccentricity of the vertical action due to differences in spans or to variable loading combinations. Nevertheless, because of roof deformability, the seismic horizontal forces acting on internal columns were proportional to the mass in their tributary areas, and therefore approximately double in internal columns with respect to those in external columns. As an example, we can compare the steel reinforcement adopted in columns in buildings n. B19 (see Figure 26) and n. B21 (Figure 10b shows a detail of the beam column connection). Building n. B19 was not designed against seismic loadings. Considering the one-floor portion of the construction, recurrent columns had rectangular (60x45 cm) cross-sections. In internal columns, the bending moment and axial force were 180 kNm and 700 kN, respectively, and columns were designed with 2Φ24 longitudinal steel bars (steel area = 90.4 mm^2) in the four corners of the column. In external columns, bending moment and axial force were 230 kNm and 600 kN, and the steel reinforcement was 2Φ24+1Φ20 (steel area = 121.8 mm^2) in the four corners. On the contrary, columns of building n. 21 were correctly designed according to seismic rules, with 60x40 cm column cross-sections. Steel reinforcement was 4Φ22 (steel area = 152.0 mm^2) along the longer sides of cross-sections in external columns and 9Φ24 (steel area = 406.8 mm^2, more than twice that of external columns) in internal columns. Considering that external columns were also stiffened by the external vertical RC cladding walls, clamped in the RC foundation beam and not considered in design, it is easy to understand why this kind of precast buildings often suffered full

internal collapses with no evident damage from outside (Figure 25b). Axial load increases in columns, caused by inertia forces produced by vertical accelerations might have contributed to these failures in near-source areas.

A very catastrophic collapse with four casualties occurred in a 9-years old precast building in Medolla (Figure 26). In this case, several negative circumstances occurred: *i*) the building was highly irregular, with two floors in the (collapsed) central part; *ii*) a heavy 15 cm thick concrete slab was cast on the top of the roof, where heavy air conditioning units were located (Figure 26 a); *iii*) the two-level portion of the building (alongside the road, top of the figure), where offices were located, had a very stiff RC staircase and many partition walls; *iv*) there was a large separation RC wall between the offices and production sections of the building. These factors contributed in making the building very irregular in plan, shifting the centroid of stiffness towards the office area. During the ground motions, large rotations occurred, with very large displacements especially on the side farthest from the road (bottom in the picture), whereas the office portion did not suffer any damage. Numerical simulations indicate that the onset of a progressive collapse is probably due to the loss of support of the upper beams on the central two-level portion of the building [43]. During the collapse, some columns failed with formation of plastic hinges at the base section (Figure 26 b, d, e), whereas others failed at the level of the intermediate slab (Figure 26 c), about 1.80 m above the corbels constituting the support of precast beams. Several columns suffered bucking of longitudinal bars (Figure 26d) with significant residual rotations. Secondary columns failed with longitudinal bar necking (Figure 26e). One column in the central portion of the building exhibited a shear – flexure failure (Figure 26f). This failure mechanism, apparently singular in such long columns, is a consequence of their peculiar design against wind actions. These columns, sustaining the two-level portion of the building, were exposed to horizontal wind loads acting only their upper part. Therefore, they were designed in order to have high moment capacity at the base but with moderate shear resistance. This is confirmed by the steel rebar detailing that can be seen in Figure 26f, i.e., seven 26 mm diameter longitudinal bars along each side of the column section and small diameter stirrups, confirming the high moment capacity and the low shear

resistance of the column. Finally, it is worth noting that, in all cases, the thick concrete industrial-pavement assured a perfect retention effect, not allowing any rotation of the columns due to foundation movements (see Section 6.3), even when they reached their full moment capacity and failed.

6.3 Failure due to movements of foundations

Some collapses of industrial buildings were due to base rotations of the columns. Even if a clear identification of the causes would require more information than what available to the authors, the collapse documented in Figure 27 can be, with a high degree of confidence, considered a consequence of the rotation of foundations. A complete absence of any cracking along the columns and the almost equal rotation of a series of columns on one side of the building, in an area where the retention action of the concrete pavement was absent, indicate a rigid rotation of the columns as the most plausible cause of collapse. This conclusion is supported by the large use, after the '90s, of pocket foundations realized with pocket precast elements simply supported over larger cast-in-situ foundations, without any connections between the two (precast and cast-in-situ) elements. In fact, in design, the verification against overturning of these foundations was performed considering wind as the only horizontal actions. Moreover, external columns usually did not exhibit any inelastic behaviour (no cracks were observed in the columns of the building in Figure 27), because their cross–sections were, in general, oversized in order to reduce the drift under wind actions (see the previous section).

6.4 Failures of external cladding panels

Several failures of external cladding panels occurred in recently designed buildings. Two different layouts of RC cladding panels walls were adopted, consisting either of horizontal or vertical panels. Horizontal cladding panels were particularly vulnerable, because of the lack of appropriate fastening devices for anchoring the panels [21] (see Figure 28). Typically, each level of cladding panels was supported by the lower level. Each panel had two connectors in its upper part, attached to specific steel profiles anchored only in the concrete cover of columns. These connectors were designed for resisting

horizontal forces orthogonal to panels, e.g., forces produced by wind pressures or seismic actions (in very recent buildings). Nevertheless, since columns exhibited large horizontal displacements in the plane of panels and panels were very stiff in plane, high relative displacement demands were produced in the connectors (especially in the upper cladding panels). It is worth noticing, that RC columns of the prefabricated structures under consideration (typically 6-8 m high in one storey structures) can feature yield drift ratios up to 1.0% - 2.0% [56,57]. As an example, consider a 1.5 m high horizontal cladding panel at a height of 5 m above ground, connected to a 50x50 cm cantilever column with typical steel reinforcement (e.g. 4 ø20mm rebars). The capacity of the column at yielding is about 250 kNm, and the relative displacement between the column (at yielding) and the top of the panel (considered undeformable) can be up to 30-35 mm. Furthermore, being the connectors for this type of panel at a distance of 1.2 m from the lower support, they must allow a relative displacement of about 10-15 mm. Since connectors were not designed to allow displacements, they were subjected to high forces that broke the steel profiles embedded in the concrete cover the columns, thus causing the failure of the cladding panels (Figure 29).

The behaviour of vertical cladding walls was better, in general. When clamped at the base on RC foundation beams and/or on concrete pavements, they also provided a significant additional stiffness and strength to the external columns of the building (Figure 25). Some collapses of vertical panels were observed, when they were not properly restrained on the foundations or when they had an internal sandwich lightweight structure (Figure 30a). In some cases, the failure of vertical panels was due to the overturning of industrial stocks contained in warehouse areas (Figure 30b).

7 DAMAGE IN WAREHOUSES

Extensive damage and collapses were observed in warehouses containing very tall racks not designed for seismic actions. The large mass of the items stocked in the racks and the large spectral acceleration for medium–long periods (see Figure 4) produced extensive collapses for this kind of structures. Furthermore, large vertical accelerations in the near-source areas might have contributed to some of the failures observed,

because of the vertical loading increase. Figure 31 shows the collapsed shelves of a warehouse for cheese curing. The lack of lateral force resisting systems and the plastic buckling of the cold formed profiles is evident in Figure 31b. The weight of the items stocked was four times larger than the weight of the building itself, and the economic value more than 20 times larger. Figure 32a shows the complete collapse of an automated warehouse containing ceramic tiles in S. Agostino. The collapsed steel structure is similar to that visible in the background on the right of the picture. Typically, these shelves were very high (over 30 meters) and, when designed without seismic provisions, without an efficient bracing system, because of the movement of machines or automated robots. Moreover, usually large weights were stocked in the upper shelves, for operational reasons.

Economic losses were very high also when automatic warehouses were only damaged by the earthquake, as in the case depicted in Figure 32b, c. In this case, the very high normal stresses in the cold-formed profiles constituting the shelve columns caused local instability and permanent deformation in the profiles (Figure 32c). The permanent displacement on the top of the shelves after the earthquake was about 20 cm. The repair and strengthening intervention of the steel structure was still possible, but it required almost one year.

8 CONCLUSIONS

The present paper documented the main damage and collapse mechanisms observed in prefabricated RC industrial buildings after the 2012 Emilia earthquakes. Buildings were classified in two main categories: *i*) buildings with double slope precast beams simply-supported at the top of columns; *ii*) buildings with flat roof, composed of long-span prestressed roof or floor elements placed on precast (prestressed or not) girder beams.

Damage and collapses in about 40 industrial buildings, covering the majority of structural typologies adopted in the area stuck by the earthquakes, were presented and illustrated, and their main causes discussed. These structures were selected from a database of 2000 buildings in which field surveys were carried out

and damage was assessed. The main causes of damage were related to the lack of seismic design requirements in the region until 2005.

The paper highlights the particular features of the ground-motions, with response spectra exhibiting high pseudo accelerations for periods in the range 0.5 – 1.0 s, and, for some of the 29th May records, a peak at 1.5 s. These ground-motions were therefore particularly severe for flexible prefabricated structures (such as structures built after the 80's). Moreover, near field effects, such as high vertical accelerations and pulse-like behaviour, were observed in some of the records produced by the accelerometric stations close to the epicentres, and might have contributed to the damage scenario. In the literature, with few exceptions, the consequences of near field phenomena have never been studied with specific reference to prefabricated structures, and might represent an interesting development for future research.

The collapse mechanisms can be classified in several different categories, depending also on the technology adopted in the period of construction. In the case of double slope roof buildings, a typology used until the eighties or for livestock shelters, the main collapse mechanisms documented are the following:

- loss of support of the roof elements from the main beams or of the main beams from columns. The interaction of portal frames with irregular masonry infill walls was often an important contributory cause. This interaction if often neglected in the current literature concerning the seismic vulnerability prefabricated structures.
- Full collapses in the case of deformable roofs, not allowing to transfer the seismic forces to the masonry panels parallel to the force direction.
- Damage for the loss of stability of the items stocked for buildings used as warehouses.

In the case of buildings with flat roof, built after the 80's for large industrial facilities, the main collapse mechanisms documented are the following:

- loss of support of the roof elements from the main beams or of the main beams from columns. The interposition of neoprene pads often even reduced the friction resistance. The in-plane flexibility of

roof also played an important role. These failures suggest that, for the proper evaluation of the seismic vulnerability of existing prefabricated buildings, it is critical to properly evaluate all the possible relative movements among prefabricated structural elements considering the stiffness and strength of mechanical connectors (when present). Future research is therefore needed to properly defined specific modelling criteria.

- Loss of lateral stability of high main beams. This kind of failure highlights the importance of evaluating overturning actions on beams in design criteria and, therefore, the need to adopt accurate numerical models to represent the geometry of prefabricated elements.
- Full collapses due to bending failure of internal columns.
- Failure of the fastening steel connections of cladding panels; in particular, it emerged that these failures were related to the large displacement demand on connectors in the plane of the cladding panels. The interaction between structural and non-structural elements was also critical, and, therefore, specific modelling and design criteria must be developed in future research.
- Damage for the loss of stability of the items stocked in warehouses.
- Rotation of foundations, in the case of pocket precast foundations not anchored to the cast-in-situ foundations.

The absence of a rigid diaphragm behaviour of roofs, remarkable for instance the case of precast elements alternated with roof-lights, strongly increased the vulnerability of these buildings, where progressive collapses often occurred.

ACKNOWLEDGEMENTS

The financial support of the (Italian) University Network of Seismic Engineering Laboratories– ReLUIS in the research program funded by the (Italian) National Civil Protection– Progetto Esecutivo 2016 – Research Line “Reinforced Concrete Structures”, WP2, is gratefully acknowledged.

REFERENCES

[1] Minghini F, Ongaretto E, Ligabue V, Savoia M, Tullini N. Observational failure analysis of precast buildings after the 2012 Emilia earthquakes. Earthquakes Struct 2016;11. doi:10.12989/eas.2016.11.2.327.

[2] Castelli V, Bernardini F, Camassi R, Caracciolo CH, Ercolani E, Postpischl E. Looking for missing earthquake traces in the Ferrara-Modena plain: an update on historical seismicity. Ann Geophys 2012;5:519–24.

[3] Lucantoni A, Bosi V, Bramerini F, De Marco R, Lo Presti T, Naso G, et al. Il rischio sismico in Italia. Ing Sismica 2001;XVIII:5–36.

[4] Presidente del Consiglio dei Ministri. OPCM 3274/2003 – Primi elementi in materia di criteri generali per la classificazione sismica del territorio nazionale e di normative tecniche per le costruzioni in zona sismica (in Italian) 2003.

[5] Italian Ministry of Public Works. Norme Tecniche per le Costruzioni (in Italian) 2008.

[6] Magliulo G, Ercolino M, Petrone C, Coppola O, Manfredi G. The Emilia Earthquake: Seismic Performance of Precast Reinforced Concrete Buildings. Earthq Spectra 2014;30:891–912. doi:10.1193/091012EQS285M.

[7] Bellotti C, Casotto C, Crowley H, Deyanova MG, Germagnoli F, Fianchisti G, et al. Single-storey precast buildings: probabilistic distribution of structural systems and subsystems from the sixties. Progett Sismica 2014;5:41–70.

[8] Bonfanti C, Carabellese A, Toniolo G. Strutture prefabbricate: catalogo delle tipologie esistenti (in Italian). 2008.

[9] Mandelli Contegni M, Palermo A, Toniolo G. Strutture prefabbricate: schedario di edifici prefabbricati in C.A. (in Italian). 2008.

[10] Nuti C, Vanzi I. Retrofitting of Industrial Structure. Int. Semin. Exhib. Recent Dev. Des. Constr.

Precast Concr. Technol. – REDECON, vol. 30, Bangalore, India, 9-14 November: 2014, p. 9–14.

[11] Ghosh SK, Cleland N. Observations from the february 27, earthquake in Chile. PCI J 2012;57:52–75.

[12] Iverson JK, Hawkins NM. Performance of Precast/Prestressed concrete building structures during Northridge Earthquake. PCI J 1994;39:38–56.

[13] Khare RK, Maniyar MM, Uma SR, Bidwai VB. Seismic performance and design of precast concrete building structures: An overview. J Struct Eng 2011;38:272–84.

[14] Muguruma H, Nishiyama M, Watanabe F. Lessons learned from the Kobe earthquake - a Japanese perspective. PCI J 1995;40:28–42.

[15] Posada M, Wood SL. Seismic Performance of Precast Industrial Buildings in Turkey. 7th US Natl Conf Earthq Eng 2002:Paper 543.

[16] Arslan MH, Korkmaz HH, Gulay FG. Damage and failure pattern of prefabricated structures after major earthquakes in Turkey and shortfalls of the Turkish Earthquake code. Eng Fail Anal 2006;13:537–57. doi:10.1016/j.engfailanal.2005.02.006.

[17] Akpinar E, Atalay HM, Ozden S, Erdogan H. Performance of precast concrete structures in October 2011 Van earthquake, Turkey. Mag Concr Res 2014;66:543–52. doi:10.1680/macr.13.00097.

[18] Toniolo G, Colombo A. Precast concrete structures: The lessons learned from the L'Aquila earthquake. Struct Concr 2012;13:73–83. doi:10.1002/suco.201100052.

[19] Savoia M, Mazzotti C, Buratti N, Ferracuti B, Bovo M, Ligabue V, et al. Damages and collapses in industrial precast buildings after the Emilia earthquake. Ingernational J Earthq Eng (Ingegneria Sismica) 2012;29:120–31.

[20] Liberatore L, Sorrentino L, Liberatore D, Decanini LD. Failure of industrial structures induced by the Emilia (Italy) 2012 earthquakes. Eng Fail Anal 2013;34:629–47. doi:10.1016/j.engfailanal.2013.02.009.

[21] Bournas DA, Negro P, Taucer FF. Performance of industrial buildings during the Emilia earthquakes

in Northern Italy and recommendations for their strengthening. Bull Earthq Eng 2013;12:2383–404. doi:10.1007/s10518-013-9466-z.

[22] Buratti N, Minghini F, Ongaretto E, Savoia M, Tullini N. Empirical seismic fragility for the precast RC industrial Buildings damaged by the 2012 Emilia (Italy) earthquakes. Submitt Publ n.d.

[23] Somerville PG. Engineering characterization of near fault ground motions. Proc. 2005 NZSEE Conf., Taupo, New Zealand, 11-13 March: 2005.

[24] Shrestha B. VERTICAL GROUND MOTIONS AND ITS EFFECT ON ENGINEERING STRUCTURES: A STATE-OF-THE-ART REVIEW. Proceeding Int. Semin. Hazard Manag. Sustain. Dev., Kathmandu, Nepal, 29-30 November: 2009. doi:10.13140/2.1.2863.6165.

[25] Grimaz S, Malisan P. Near field domain effects and their consideration in the international and Italian seismic codes. Boll Di Geofis Teor Ed Appl 2014;55:717–38. doi:10.4430/bgta0130.

[26] Li S, Xie L. Progress and trend on near-field problems in civil engineering. Acta Seismol Sin 2007;20:105–14. doi:10.1007/s11589-007-0105-0.

[27] Pondrelli S, Salimbeni S, Ekström G, Morelli A, Gasperini P, Vannucci G. The Italian CMT dataset from 1977 to the present. Phys Earth Planet Inter 2006;159:286–303. doi:10.1016/j.pepi.2006.07.008.

[28] Rovida A, Camassi R, Gasperini P, Stucchi M. CPTI11, the 2011 version of the Parametric Catalogue of Italian Earthquakes. Milan/Bologna: 2001.

[29] Boccaletti M, Corti G, Martelli L. Recent and active tectonics of the external zone of the Northern Apennines (Italy). Int J Earth Sci 2011;100:1331–48. doi:10.1007/s00531-010-0545-y.

[30] Pieri M, Groppi G. Subsurface geological structure of the Po Plain, Italy. C.N.R. (Italian National Council for Research); 1981.

[31] Ori GG, Friend PF. Sedimentary basins formed and carried piggyback on active thrust sheets. Geology 1984;12:475–8. doi:10.1130/0091-7613(1984)12<475:sbfacp>2.0.co;2.

[32] Zerbini S, Matonti F, Doglioni C. Crustal movements in northeastern Italy from permanent GPS

stations. Geophys. Res. Abstr. Proc. Eur. Geosci. Union 2006, vol. 8, Vienna, Austria: 2006, p. 6257.

[33] Devoti R, Pierantonio G, Pisani A, Riguzzi F, Serpelloni E. Present day kinematics of Italy. J Virtual Explor 2010;36. doi:10.3809/jvirtex.2010.00237.

[34] Gorini A, Nicoletti M, Marsan P, Bianconi R, Nardis R, Filippi L, et al. The Italian strong motion network. Bull Earthq Eng 2010;8:1075–90. doi:10.1007/s10518-009-9141-6.

[35] Di Capua G, Lanzo G, Pessina V, Peppoloni S, Scasserra G. The recording stations of the Italian strong motion network: geological information and site classification. Bull Earthq Eng 2011;9:1779–96. doi:10.1007/s10518-011-9326-7.

[36] Pacor F, Paolucci R, Ameri G, Massa M, Puglia R. Italian strong motion records in ITACA: overview and record processing. Bull Earthq Eng 2011;9:1741–59. doi:10.1007/s10518-011-9295-x.

[37] Pacor F, Paolucci R, Luzi L, Sabetta F, Spinelli A, Gorini A, et al. Overview of the Italian strong motion database ITACA 1.0. Bull Earthq Eng 2011;9:1723–39. doi:10.1007/s10518-011-9327-6.

[38] Paolucci R, Pacor F, Puglia R, Ameri G, Cauzzi C, Massa M. Record Processing in ITACA, the New Italian Strong-Motion Database. In: Akkar S, Gülkan P, van Eck T, editors. Earthq. Data Eng. Seismol. - Predict. Model. Data Manag. Networks, Springer Netherlands; 2011.

[39] Bozzoni F, Lai CG, Scandella L. Preliminary results of ground-motion characteristics. Ann Geophys 2012;55:609–14.

[40] Priolo E, Romanelli M, Barnaba C, Mucciarelli M, Laurenzano G, Dall'Olio L, et al. The Ferrara thrust earthquakes of May-June 2012: preliminary site response analysis at the sites of the OGS temporary network. Ann Geophys 2012;55:591–7.

[41] Ohori M, Nobata A, Wakamatsu K. A Comparison of ESAC and FK Methods of Estimating Phase Velocity Using Arbitrarily Shaped Microtremor Arrays. Bull Seismol Soc Am 2002;92:2323–32. doi:10.1785/0119980109.

[42] Gallipoli MR, Chiauzzi L, Stabile TA, Mucciarelli M, Masi A, Lizza C, et al. The role of site effects in the comparison between code provisions and the near field strong motion of the Emilia 2012

earthquakes. Bull Earthq Eng 2014;12:2211–30. doi:10.1007/s10518-014-9628-7.

[43] Bovo M, Savoia M. Numerical simulation of seismic-induced failure of a precast structure during the Emilia earthquake. Manuscript Submitted for Publication.

[44] Magliulo G, Ercolino M, Manfredi G. Influence of cladding panels on the first period of one-story precast buildings. Bull Earthq Eng 2015;13:1531–55. doi:10.1007/s10518-014-9657-2.

[45] Biondini F, Titi A, Toniolo G. Prestazioni sismiche di strutture prefabbricate con connessioni trave-pilastro ad attrito. Proc. XV Conf. Ital. Assoc. Seism. Eng., Padua, Italy, 30 June - 4 July: 2013.

[46] Baker JW. Quantitative Classification of Near-Fault Ground Motions. Bull Seismol Soc Am 2007;97:1486–501.

[47] Mavroeidis GP, Dong G, Papageorgiou AS. Near-fault ground motions, and the response of elastic and inelastic single-degree-of-freedom (SDOF) systems. Earthq Eng Struct Dyn 2004;33:1023–49.

[48] MacRae GA, Morrow D V., Roeder CW. Near-Fault Ground Motion Effects on Simple Structures. J Struct Eng 2001;127:996–1004. doi:10.1061/(ASCE)0733-9445(2001)127:9(996).

[49] Italian Ministry of Public Works. D.M. 16/1/1996 - Norme Tecniche relative alle costruzioni in zona sismica 1996.

[50] Italian National Research Council - CNR. Istruzioni per il progetto, l'esecuzione e il controllo delle strutture prefabbricate in conglomerate cementizio e per le strutture costruite con sistemi industrializzati – CNR 10025 (in Italian) 1984.

[51] Italian Ministry of Public Works. D.M. 3/12/1987 – Norme tecniche per la progettazione, esecuzione e collaudo delle costruzioni prefabbricate 1987.

[52] Ministro dei Lavori Pubblici. D.M. 14/2/1992 - Norme tecniche per l'esecuzione delle opere in cemento armato normale e precompresso e per le strutture metalliche 1992.

[53] Italian Ministry of Public Works. D.M. 9.1.1996 – Norme Tecniche per il calcolo, l'esecuzione ed il collaudo delle strutture in cemento armato, normale e precompresso e per le strutture metalliche (in Italian) 1996.

[54] FIB. Model Code for Concrete Structures 2010. Ernst & Shon; 2013.

[55] Magliulo G, Capozzi V, Fabbrocino G, Manfredi G. Neoprene–concrete friction relationships for seismic assessment of existing precast buildings. Eng Struct 2011;33:532–8. doi:10.1016/j.engstruct.2010.11.011.

[56] Ercolino M, Magliulo G, Manfredi G. Failure of a precast RC building due to Emilia-Romagna earthquakes. Eng Struct 2016;118:262–73. doi:10.1016/j.engstruct.2016.03.054.

[57] Panagiotakos TB, Fardis MN. Deformations of Reinforced Concrete Members at Yielding and Ultimate. ACI Struct J 2001;98:135.

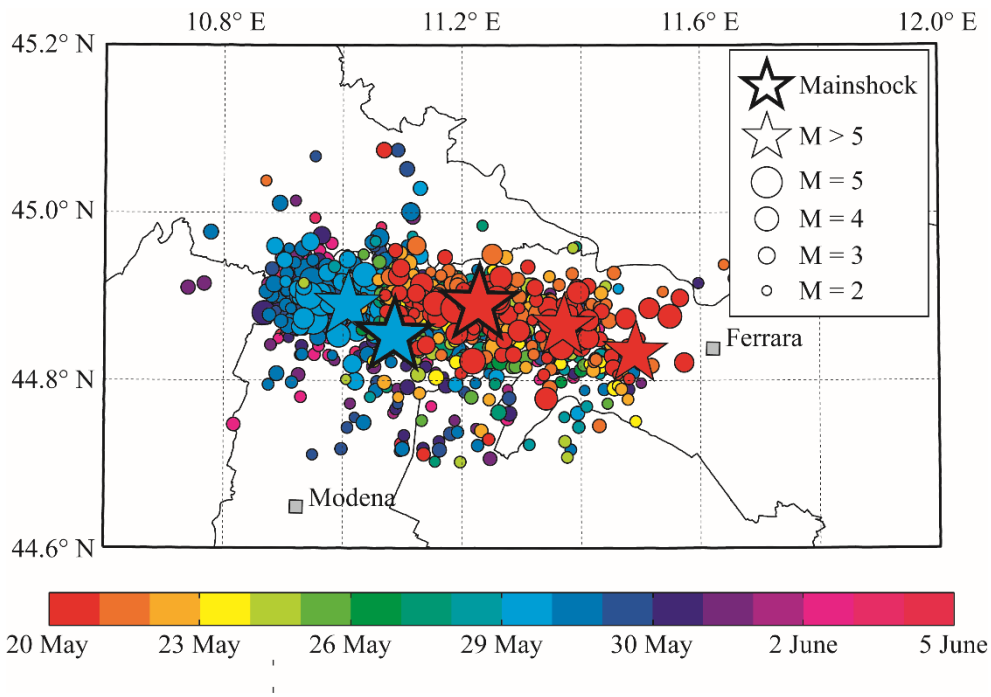
10.8° E
11.2° E
11.6° E
12.0° E
45.2° N
45.0° N
44.8° N
44.6° N
Mainshock
M > 5
M = 5
M = 4
M = 3
M = 2
Ferrara
Modena
20 May
23 May
26 May
29 May
30 May
2 June
5 June

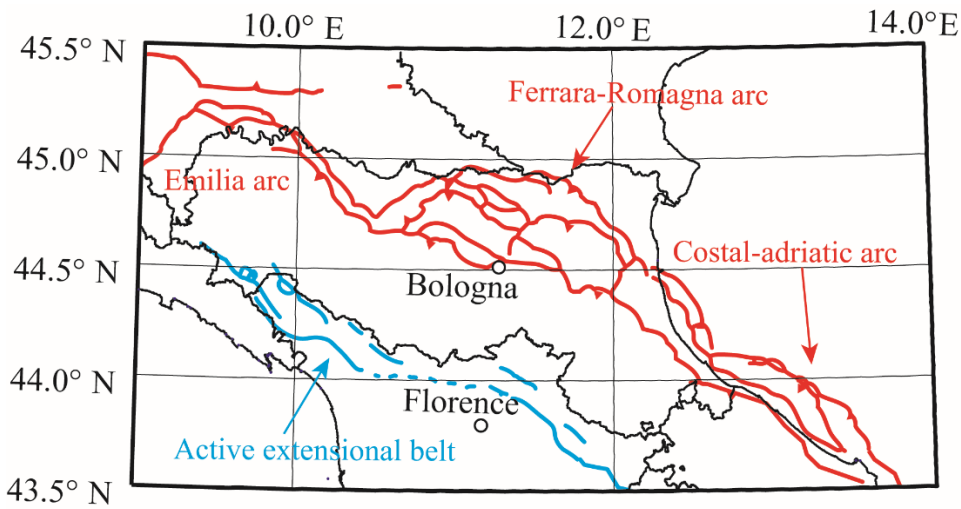
10.0° E
12.0° E
14.0°E
45.5° N
45.0° N
44.5° N
44.0° N
43.5° N
Ferrara-Romagna arc
Emilia arc
Costal-adriatic arc
Bologna
Florence
Active extensional belt

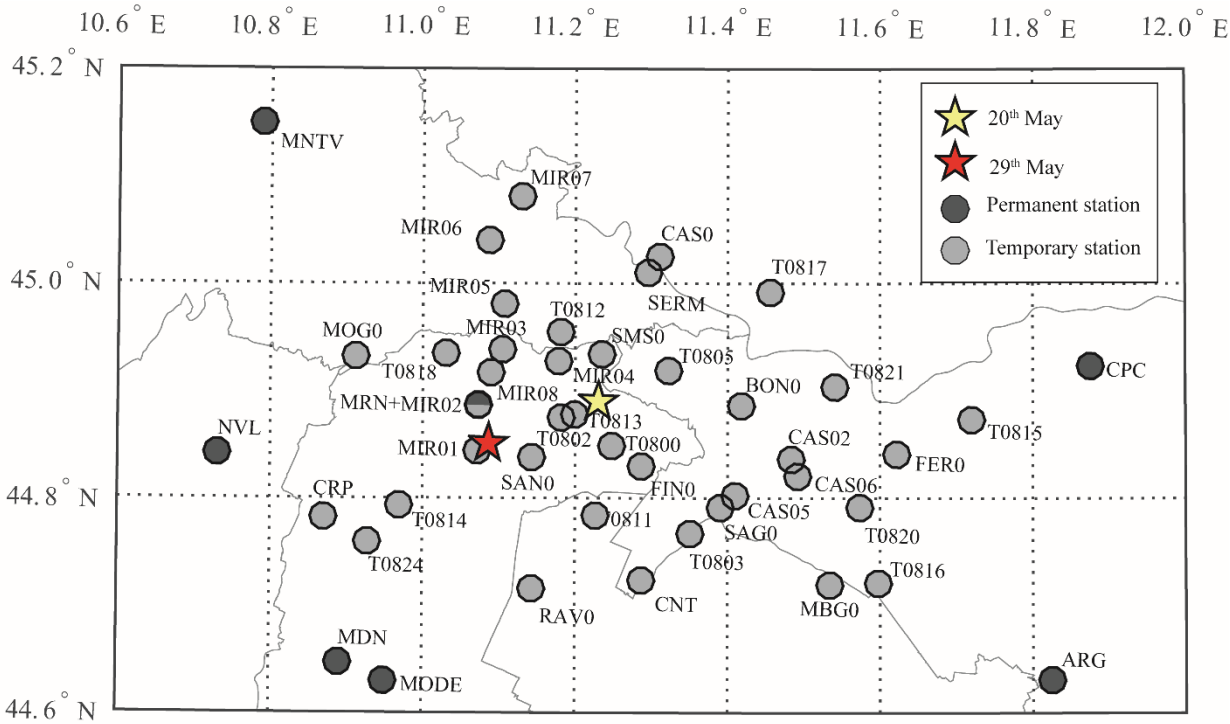
10.6° E
10.8° E
11.0° E
11.2° E
11.4° E
11.6° E
11.8° E
12.0° E
45.2° N
45.0° N
44.8° N
44.6° N
20th May
29th May
Permanent station
Temporary station
MNTV
MIR07
MIR06
CAS0
T0817
MIR05
T0812
SERM
MOG0
MIR03
SMS0
T0805
T0818
MIR04
T0821
CPC
MIR08
BON0
MRN+MIR02
T0813
NVL
T0815
MIR01
T0802
T0800
CAS02
FER0
SAN0
FIN0
CAS06
CRP
CAS05
T0814
T0811
SAG0
T0820
T0824
T0803
T0816
RAV0
CNT
MBG0
MDN
ARG
MDDE

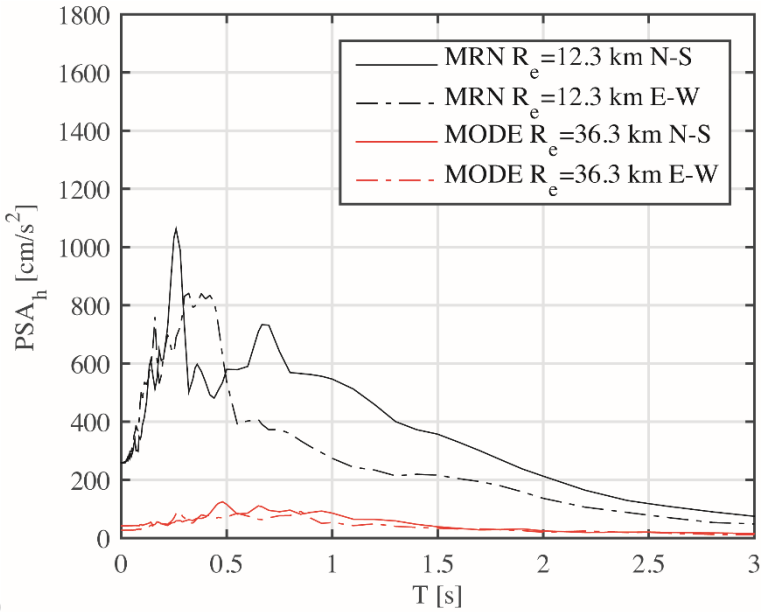
MRN R_e=12.3 km N-S
MRN R_e=12.3 km E-W
MODE R_e=36.3 km N-S
MODE R_e=36.3 km E-W
PSA_h [cm/s^2]
T [s]
0
200
400
600
800
1000
1200
1400
1600
1800
0.5
1
1.5
2
2.5
3

a)

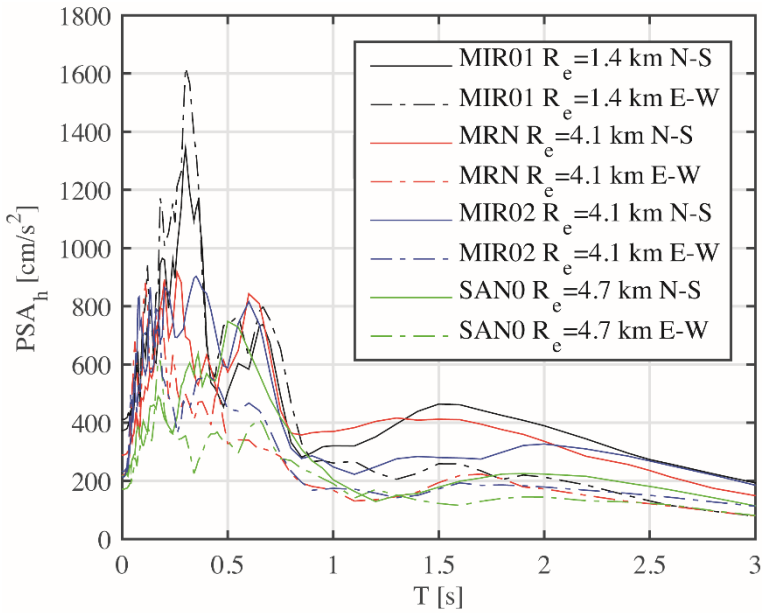
MIR01 R_e=1.4 km N-S
MIR01 R_e=1.4 km E-W
MRN R_e=4.1 km N-S
MRN R_e=4.1 km E-W
MIR02 R_e=4.1 km N-S
MIR02 R_e=4.1 km E-W
SAN0 R_e=4.7 km N-S
SAN0 R_e=4.7 km E-W
PSA_h [cm/s^2]
T [s]
0
200
400
600
800
1000
1200
1400
1600
1800
0.5
1
1.5
2
2.5
3

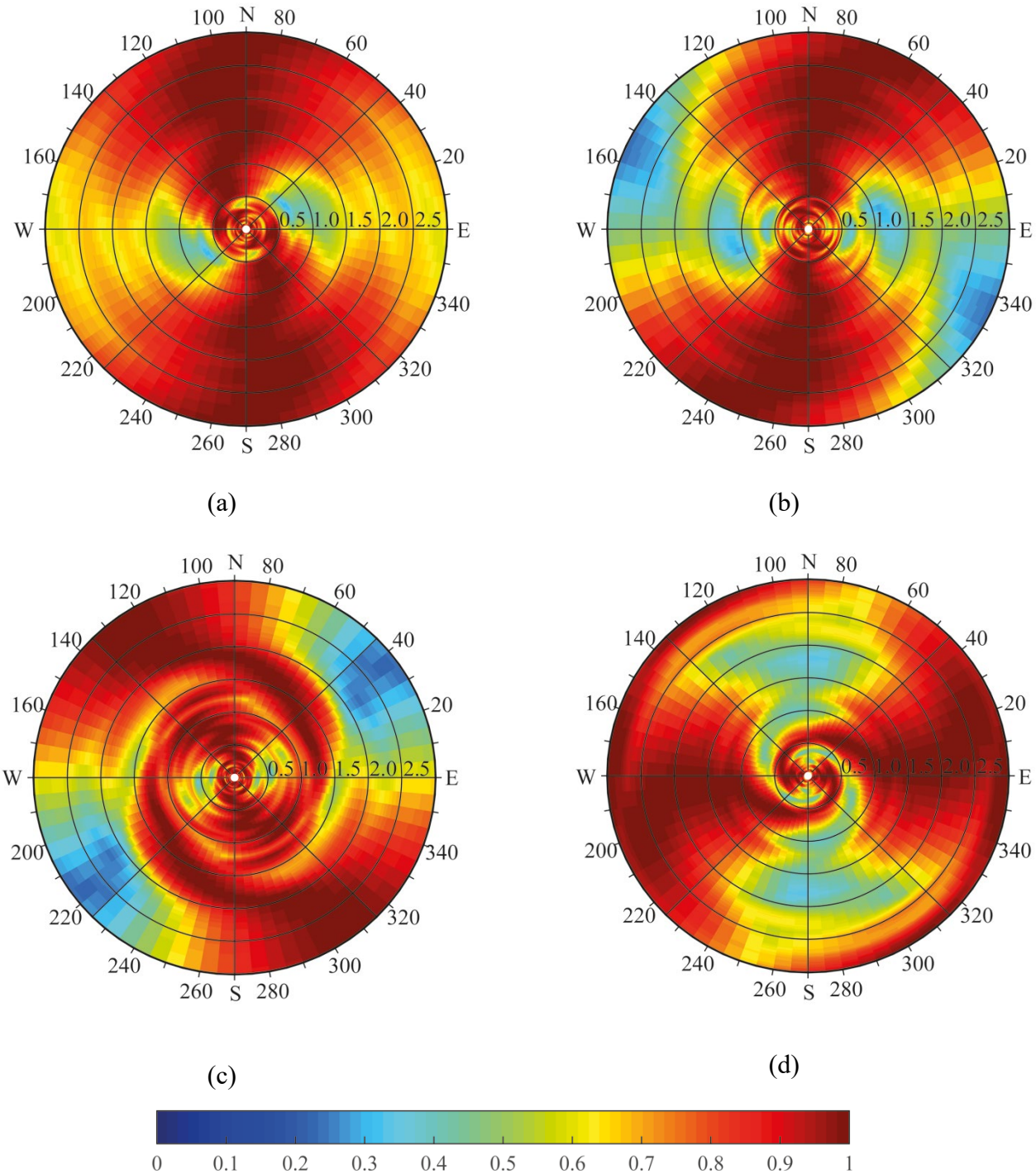

Figure 5. Directionality of PSA_h. May 20th earthquake: (a) at MRN (R_e = 12.3 km) station, May 29th earthquake: (b) MRN (R_e = 4.1 km), (c) SAN0 (R_e = 4.7 km) and (d) T0800 (R_e = 12.8 km) stations. The angles indicate the orientation of a SDOF system with respect to East, Different natural periods are reported (in s) on the radial axis. The colour scale indicates the ratio, for each period, of the PSA_h at the general orientation over the maximum PSA_h among all orientations. See Figure 3 for station locations.

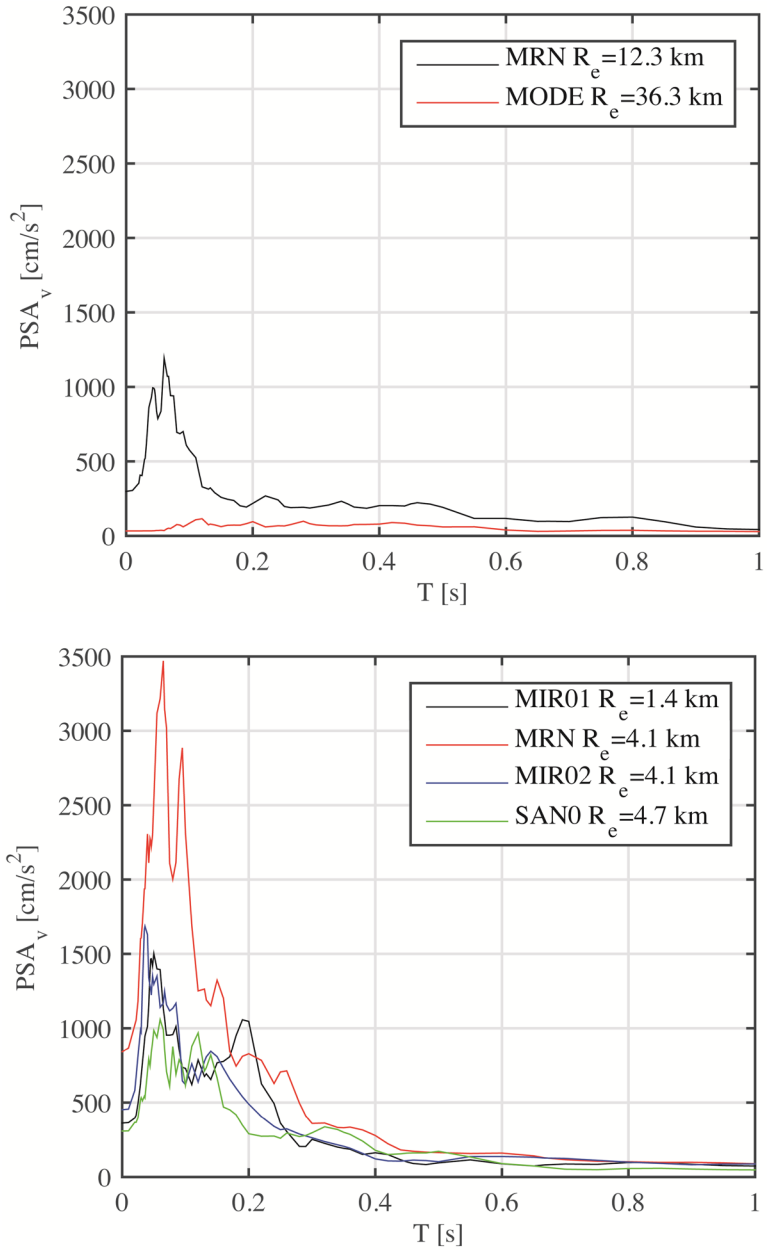

Figure 6. Pseudo-acceleration response spectra for the vertical ground motion component recorded at the stations closest to the epicentres of the (a) May 20th and (b) May 29th earthquakes.

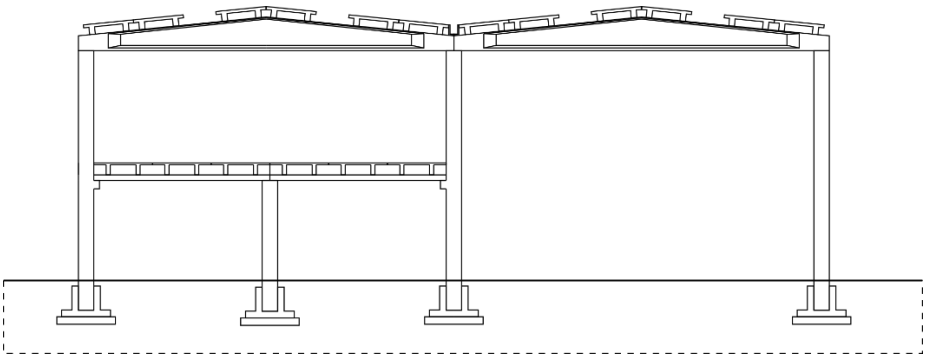

(a)

(b)

Figure 7. Precast building with double slope roof beams (Type 1) and masonry infills, between beams and columns, carrying the horizontal loadings.

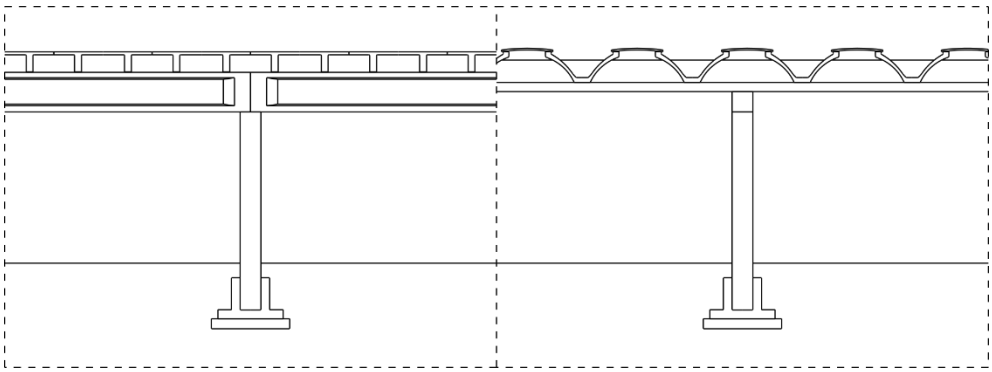

(a)

(b)

Figure 8. (a) Precast buildings with planar roof (Type 2) and (b) long prestressed omega-shaped girders with thin-web roof elements for a production area. In the picture, the detail of a safety intervention executed before restart the working activity is also shown.

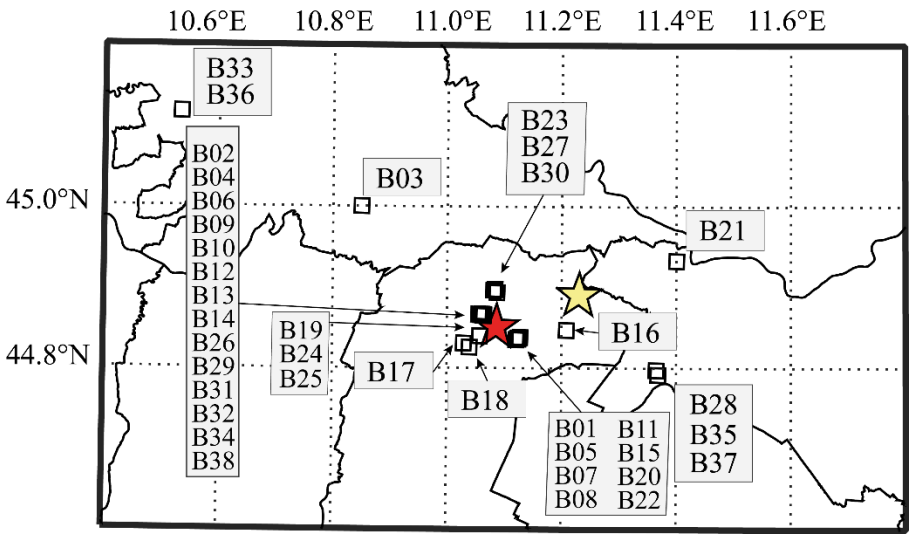

Figure 9. Locations of the buildings described in the paper. See Figure 1 for further information on epicentres.

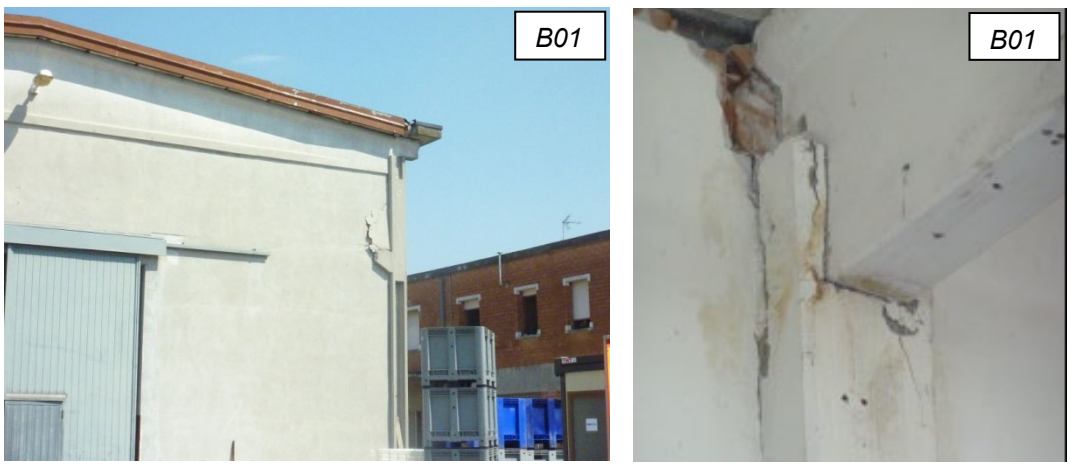

Figure 10. (a) Precast RC building with regular masonry cladding walls, only slightly damaged by the earthquake; (b) Damage to the column fork, due to the transverse rotation of the double slope roof beam during the ground motion.

(a)

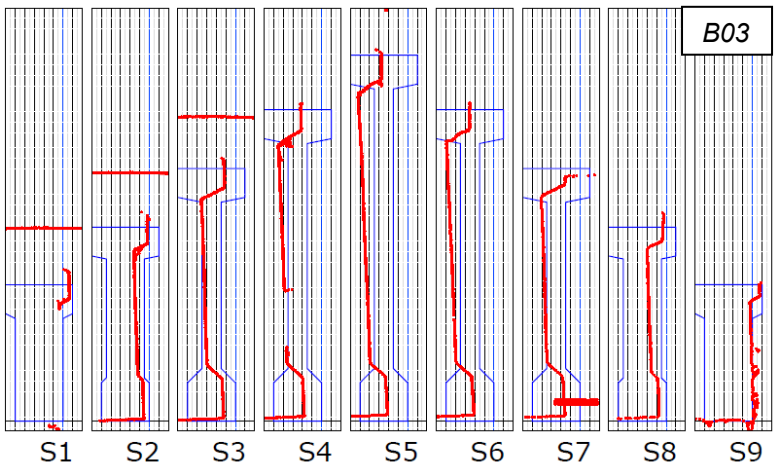

(b)

Figure 11: (a) A collapsed building with deformable roof, the only remaining elements are the two short facade masonry walls; (b) permanent rotation after the earthquake of different cross sections of a double-slope beam. S1 and S9 are the support sections and S5 at mid-span. Blue and red lines indicate the theoretical and the actual position, respectively.

Figure 12: (a, b, c) Collapses due to the presence of strip windows on the top of masonry walls (the building in picture (a) is the same shown in Figure 7b before the collapse); (d) collapse due to the presence of an internal masonry wall (indicated by an arrow).

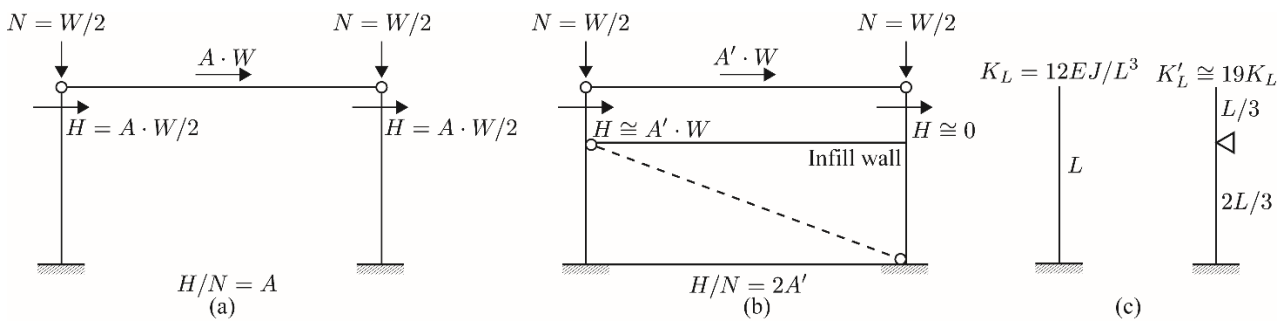

Figure 13: Short column effect in a terminal frame with infill walls and a strip window: a) a central frame without infill wall; b) an infilled frame with strip window;c) stiffness variation due to the short column effect.

(a)

(b)

(c)

Figure 14. Flexural-shear (a) and flexural (b, c) damage of the facade columns due to the interaction with irregular masonry walls.

Figure 15. Collapse of the beam of the facade frame due to the interaction with the non structural columns indicated with an arrow.

(a)

(b)

Figure 16: Collapses due to plan-irregularities in two industrial buildings.

Figure 17. (a) Out-of-plane collapse of a cladding masonry wall non properly connected to the top beam due to the presence of a strip windows; (b) partial roof collapse in a curved roof due to the interaction with the masonry façade panels.

Figure 18. Complete collapse of a recently built precast structure.

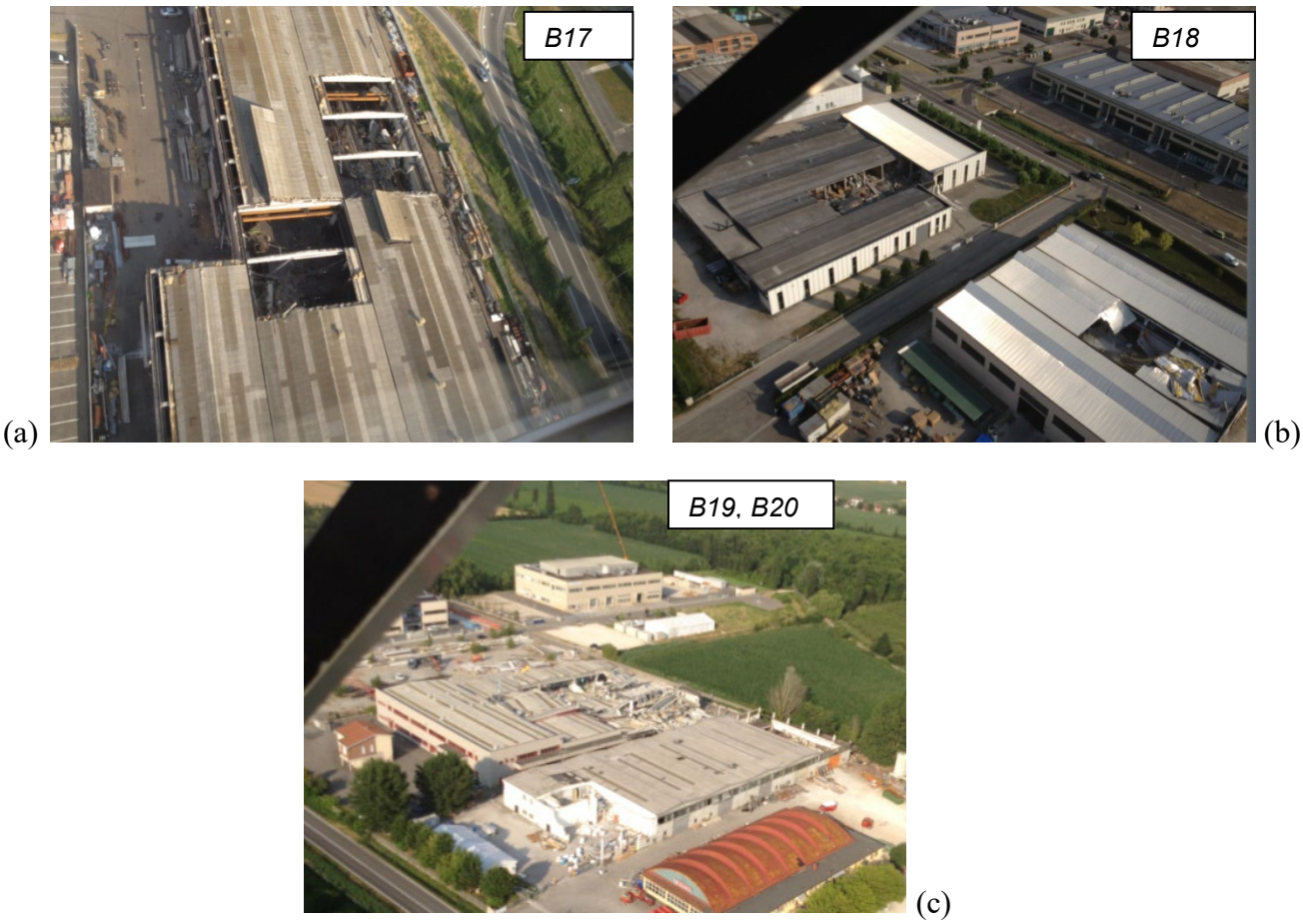

Figure 19. Failures of roof elements, often located in irregular portion of buildings.

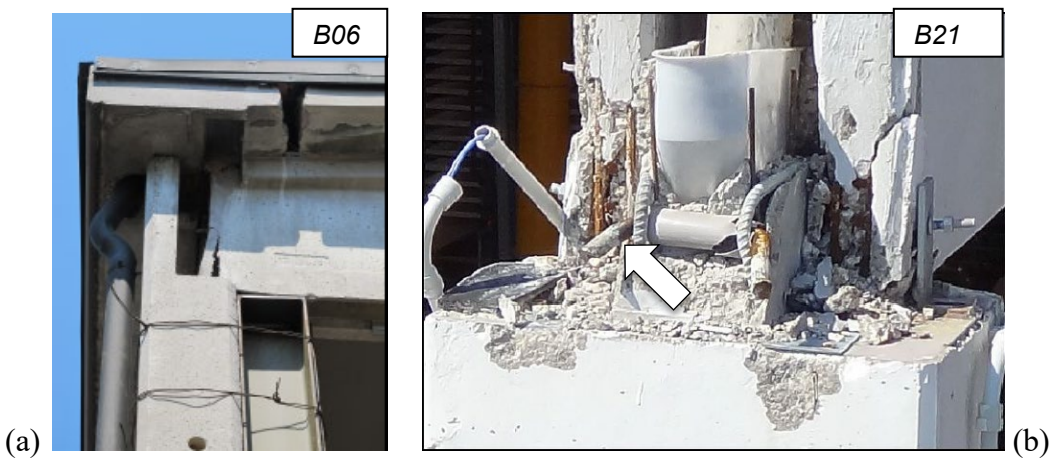

Figure 20. (a) Damage at the extremity of a precast beam where no steel rebars were present in the beam to carry the force transferred by the steel dowel in the beam - column connection; (b) the steel dowel completely bent because unable to carry the horizontal force at the beam – column connection.

Figure 21: Collapses in a recent fruit warehouse with inclined precast beams to realize a shed structure.

Figure 22. Failure due to the loss of support of roof elements related to plan-irregularity a commercial prefabricated building.

Figure 23. Complete collapse of and industrial building due to lateral overturning of beams.

(a)

(b)

Figure 24. (a, b) Permanent lateral beam rotations in two partially collapsed buildings.

(a)

(b)

Figure 25. Complete collapse of two industrial buildings due to the failure of the internal columns.

Figure 26. A collapsed building in Cavezzo (MO): (a) Aerial view, (b) column rotation due to the formation of a flexural plastic hinge, (c) rupture of a column in an intermediate position due to the presence of a TT precast slab, (d) plastic hinge with bar instability, (e) flexural failure with bar necking, (f) shear failure of a highly reinforced column in flexure.

Figure 27. Complete collapses of an industrial building in S. Agostino, with large base rotations of the columns probably due to rotation of foundations.

(a)

(b)

(b)

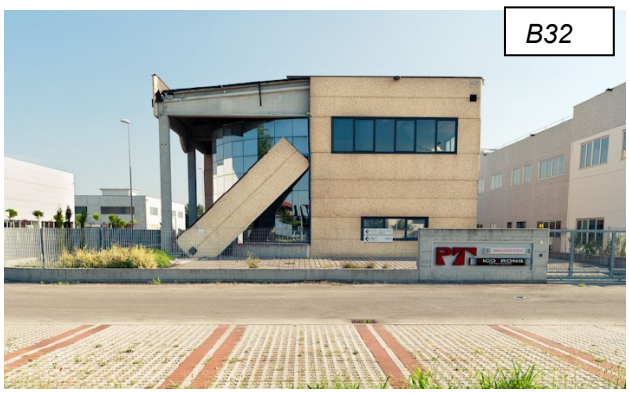

(d)

Figure 28. (a – d) Collapse of horizontal precast cladding panels.

(a)

(b)

(c)

Figure 29. Damage of fastening devices for panel- column connections when their deformation capacity was exceeded.

(a)

(b)

Figure 30. Collapse of precast cladding panels non properly restrained at the base.

(a)

(b)

Figure 31. (a) Collapse of a cheese warehouse in the province of Mantova, (b) detail of the light steel structure made of cold-formed steel profiles not designed to bear horizontal loads.

(a)

(b) 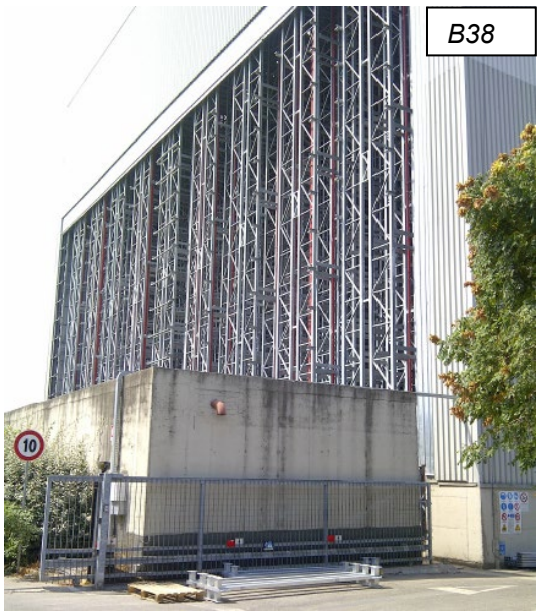

(c)

Figure 32. (a) Collapse of an automated warehouse containing ceramic tiles; (b, c) an automatic warehouse with permanent deformations after the earthquake, and detail of plastic bucking in a column after dismounting.

Table 1. Ground-motion records classified as pulse-like according to the criterion proposed by Baker [46]. *For each record the table reports the epicentral distance, the recording station (see Figure 3), the orientation, the Peak Ground Velocity (PGV), and the pulse-period T_p.*

Event	Epicentral Distance [km]	Station	Component	PGV [cm/s]	T_p [s]
20 May	12.3	MRN	N-S	46.3	1.80
29 May	1.4	MIR01	N-S	52.4	2.63
29 May	4.1	MRN	N-S	57.5	2.50
29 May	4.1	MIR02	E-W	36.4	2.79
29 May	4.7	SAN0	N-S	35.3	2.47
29 May	11.2	MIR04	N-S	35.4	0.81